

## Diluted II-VI Oxide Semiconductors with Multiple Band Gaps

K. M. Yu,<sup>1</sup> W. Walukiewicz,<sup>1</sup> J. Wu,<sup>1</sup> W. Shan,<sup>1</sup> J.W. Beeman,<sup>1</sup> M. A. Scarpulla,<sup>1,2</sup> O. D. Dubon,<sup>1,2</sup> and P. Becla<sup>3</sup>

<sup>1</sup>*Materials Sciences Division, Lawrence Berkeley National Laboratory, Berkeley, California 94720, USA*

<sup>2</sup>*Department of Materials Science and Engineering, University of California, Berkeley, California 94720, USA*

<sup>3</sup>*Department of Materials Science and Engineering, Massachusetts Institute of Technology, Cambridge, Massachusetts 02139, USA*

(Received 24 July 2003; published 11 December 2003)

We report the realization of a new mult-band-gap semiconductor.  $Zn_{1-y}Mn_yO_xTe_{1-x}$  alloys have been synthesized using the combination of oxygen ion implantation and pulsed laser melting. Incorporation of small quantities of isovalent oxygen leads to the formation of a narrow, oxygen-derived band of extended states located within the band gap of the  $Zn_{1-y}Mn_yTe$  host. When only 1.3% of Te atoms are replaced with oxygen in a  $Zn_{0.88}Mn_{0.12}Te$  crystal the resulting band structure consists of two direct band gaps with interband transitions at  $\sim 1.77$  and 2.7 eV. This remarkable modification of the band structure is well described by the band anticrossing model. With multiple band gaps that fall within the solar energy spectrum,  $Zn_{1-y}Mn_yO_xTe_{1-x}$  is a material perfectly satisfying the conditions for single-junction photovoltaics with the potential for power conversion efficiencies surpassing 50%.

DOI: 10.1103/PhysRevLett.91.246403

PACS numbers: 71.20.Nr, 61.72.Vv, 78.66.Hf, 89.30.Cc

Recently a new class of semiconductors has emerged, whose fundamental properties are dramatically modified through the substitution of a relatively small fraction of host atoms with an element of very different electronegativity, the so called highly mismatched alloys (HMAs). III-V and II-VI alloys, in which group V and VI anions are replaced with the isovalent N [1] and O [2], respectively, are the well-known examples of the HMAs. For example,  $GaN_xAs_{1-x}$  exhibits a strong reduction of the band gap by 180 meV when only 1% of the As atoms is replaced by N [1].

The unusual properties of HMAs are well explained by the recently developed band anticrossing (BAC) model [3–5]. The model has also predicted several new effects that were later confirmed by experiments [6–8]. According to this model the electronic structure of the HMAs is determined by the interaction between localized states associated with N or O atoms and the extended states of the host semiconductor matrix. As a result the conduction band splits into two subbands with distinctly nonparabolic dispersion relations [3].

In most instances, e.g., N in GaAs or O in CdTe, the localized states are located within the conduction band and the anticrossing interaction results in the formation of a relatively wide lower subband [5]. The subband is shifted to lower energies leading to a reduction of the energy band gap. The BAC model predicts that a narrow band can be formed only if the localized states occur well below the conduction band edge. Such a case is realized in ZnTe, MnTe, and  $Zn_{1-y}Mn_yTe$  alloys where the O level is located roughly 0.2 eV below the conduction band edge.

We have shown recently that pulsed laser melting (PLM) followed by rapid thermal annealing (RTA) is well suited for the synthesis of HMAs. The rapid recrystallization rate associated with the PLM process results in the incorporation of impurity atoms to a level

well above the solubility limit [9,10]. The combined ion beam and laser processing approach has been demonstrated as an effective approach to synthesize dilute semiconductor alloys including  $GaN_xAs_{1-x}$  [11,12] and  $Ga_{1-x}Mn_xAs$  [13].

Here we report the synthesis of a new type of material, the highly mismatched  $Zn_{1-y}Mn_yO_xTe_{1-x}$  that has a narrow band of extended states within a semiconductor band gap using O ion implantation followed by PLM. This material satisfies the criteria for a multiband semiconductor and could be used to test the theoretical predictions of enhanced solar cell efficiency. The design of our material is based on the BAC model of highly mismatched semiconductor alloys (HMAs).

Multiple energy implantation using 90 and 30 keV  $O^+$  was carried out into  $Zn_{1-y}Mn_yTe$  ( $y = 0$  and 0.12) single crystals to form  $\sim 0.2 \mu\text{m}$  thick layers with relatively constant O concentrations corresponding to O mole fractions of 0.0165–0.044. The  $O^+$ -implanted samples were pulsed laser melted in air using a KrF laser ( $\lambda = 248 \text{ nm}$ ) with a FWHM pulse duration  $\sim 38 \text{ ns}$  [12]. After passing through a multiprism homogenizer, the fluence at the sample ranged between 0.020 and 0.3  $\text{J}/\text{cm}^2$ . Some of the samples underwent RTA after the PLM at temperatures between 300 and 700 °C for 10 sec in flowing  $N_2$ .

The band gap of the films was measured at room temperature using photomodulated reflectance (PR). Radiation from a 300 W halogen tungsten lamp dispersed by a 0.5 m monochromator was focused on the samples as a probe beam. A chopped HeCd laser beam ( $\lambda = 442$  or 325 nm) provided the photomodulation. PR signals were detected by a Si photodiode using a phase-sensitive lock-in amplification system. The values of the band gap and the linewidth were determined by fitting the PR spectra to the Aspnes third-derivative functional form [14].

Figure 1 shows a series of PR spectra from  $\text{Zn}_{0.88}\text{Mn}_{0.12}\text{Te}$  samples implanted with 3.3% of  $\text{O}^+$  followed by PLM with increasing laser energy fluence from 0.04 to 0.3  $\text{J}/\text{cm}^2$ . Two optical transitions at  $\sim 1.8$  and 2.6 eV, distinctly different from the fundamental band gap transition ( $E_M = 2.32$  eV) of the matrix, can be clearly observed from the samples after PLM with fluences  $\geq 0.08$   $\text{J}/\text{cm}^2$ . Identical PLM treatments on unimplanted and  $\text{Ne}^+$ -implanted  $\text{ZnMnTe}$  samples do not show such transitions, indicating that they are not caused by the implantation damage. These results suggest that  $\text{Zn}_{0.88}\text{Mn}_{0.12}\text{O}_x\text{Te}_{1-x}$  layers are formed after  $\text{O}^+$  implantation and PLM with energy fluence  $\geq 0.08$   $\text{J}/\text{cm}^2$ . The two optical transitions can be attributed to transitions from the valence band to the two conduction subbands,  $E_+$  ( $\sim 2.6$  eV) and  $E_-$  ( $\sim 1.8$  eV) formed as a result of the hybridization of the localized O states and the extended conduction band states of  $\text{ZnMnTe}$ . The strong signals at both  $E_-$  and  $E_+$  indicates the extended nature of these electronic states and the substantial oscillator strength for the transitions.

The BAC model suggests that the two level interaction leads to the upward shift of the upper state and the downward shift of the lower state by exactly the same energy equal to  $\frac{1}{2}[\sqrt{(E_a - E_b)^2 + 4C_{LM}^2x} - E_a - E_b]$ , where  $E_a$  and  $E_b$  are the original energy levels (in this case  $E_M$

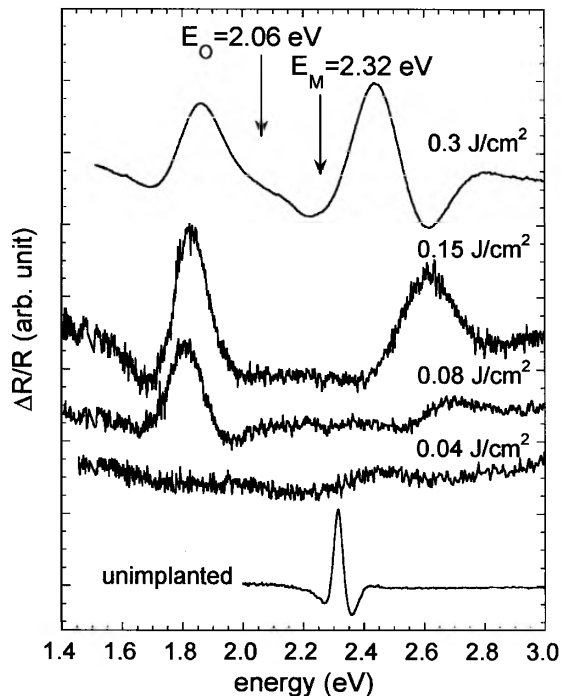


FIG. 1. Photomodulated reflectance (PR) spectra obtained from a series of 3.3%  $\text{O}^+$ -implanted  $\text{Zn}_{0.88}\text{Mn}_{0.12}\text{Te}$  samples followed by pulsed laser melting with increasing energy fluence from 0.04–0.3  $\text{J}/\text{cm}^2$ . The PR spectrum from an as-grown  $\text{Zn}_{0.88}\text{Mn}_{0.12}\text{Te}$  crystal is also shown for comparison.

and  $E_0$ ), and  $C_{LM}$  is the matrix element describing the coupling between localized states and the extended states [3–5]. From the known values of the band offset of  $\text{ZnTe}$  and  $\text{MnTe}$  and the energy level of O in  $\text{ZnTe}$  [15], the O level is estimated to be at 2.06 eV with respect to the valence band maximum for  $\text{Zn}_{0.88}\text{Mn}_{0.12}\text{Te}$ . The PR spectrum from the sample PLM with 0.15  $\text{J}/\text{cm}^2$  shown in Fig. 1 indicates very similar energy shifts ( $E_0 - E_-$ ) = 0.234 eV and ( $E_+ - E_M$ ) = 0.24 eV. This is in perfect agreement with the prediction of the BAC model. Notice also that the transitions at around 2.6 eV shown in Fig. 1 are the first observation of the  $E_+$  subband in II-VI HMAAs.

For  $\text{GaN}_x\text{As}_{1-x}$  and  $\text{ZnSe}_x\text{Te}_{1-x}$  the values of the coupling parameter  $C_{LM}$  have been determined to be 2.7 and 1 eV, respectively [3,4]. Since it is believed that the magnitude of  $C_{LM}$  depends on the electronegativity difference ( $\Delta\chi$ ) between the matrix anion elements, and this difference is larger between O and Te ( $\Delta\chi = 1.4$ ) than that between N and As ( $\Delta\chi = 1.0$ ), we make the assumption that  $C_{LM} \approx 3.5$  eV in  $\text{ZnMnTe}$ . The substitutional O content of the  $\text{Zn}_{0.88}\text{Mn}_{0.12}\text{O}_x\text{Te}_{1-x}$  alloys formed by  $\text{O}^+$  implantation followed by PLM with 0.15  $\text{J}/\text{cm}^2$  shown in Fig. 1 is estimated to be  $x \approx 0.01$ .

We have reported previously that in the formation of  $\text{Cd}_{1-y}\text{Mn}_y\text{O}_x\text{Te}_{1-x}$  alloys by  $\text{O}^+$  implantation and RTA, Mn leads to increased stability of substitutional O in  $\text{Cd}_{1-y}\text{Mn}_y\text{Te}$  [2]. In the present Letter we have also demonstrated the formation of  $\text{ZnO}_x\text{Te}_{1-x}$  layers with  $x \sim 0.01$  by  $\text{O}^+$  implantation and PLM (data not shown). We believe that the role of Mn in stabilizing O in the Te sublattice is suppressed because of the rapid epitaxial regrowth rate of the PLM process estimated to be on the order of meters per second.

Figure 2 shows a series of PR spectra from the 3.3%  $\text{O}^+$ -implanted  $\text{Zn}_{0.88}\text{Mn}_{0.12}\text{Te}$  samples after PLM with fluence = 0.15  $\text{J}/\text{cm}^2$  followed by RTA for 10 s at temperatures between 300 and 700  $^\circ\text{C}$ . A reduction in the energy shifts of both  $E_-$  and  $E_+$  can be observed at RTA temperature higher than 350  $^\circ\text{C}$ . This indicates that the  $\text{Zn}_{0.88}\text{Mn}_{0.12}\text{O}_x\text{Te}_{1-x}$  alloys are thermally stable up to  $\sim 350$   $^\circ\text{C}$ . At an RTA temperature of 700  $^\circ\text{C}$ , only the original  $E_M$  transition is observed. This may suggest that the O atoms that resided in the Te sites diffused out of the Te sites, possibly forming O bubbles [12]. It is also worth noting that the BAC model predicts that as the  $E_-$  transition approaches the localized O level, as in the case of the samples after RTA at temperatures between 400 and 555  $^\circ\text{C}$ , the nature of the lowest subband minimum becomes more localized. This can account for the observed broadening of the transition in Fig. 2.

The energy positions of  $E_-$  and  $E_+$  for the  $\text{Zn}_{0.88}\text{Mn}_{0.12}\text{O}_x\text{Te}_{1-x}$  alloys with different  $x$  are plotted in Fig. 3. Data are taken from samples implanted with different amounts of O [(1.65, 2.2, and 4.4)%] as well as

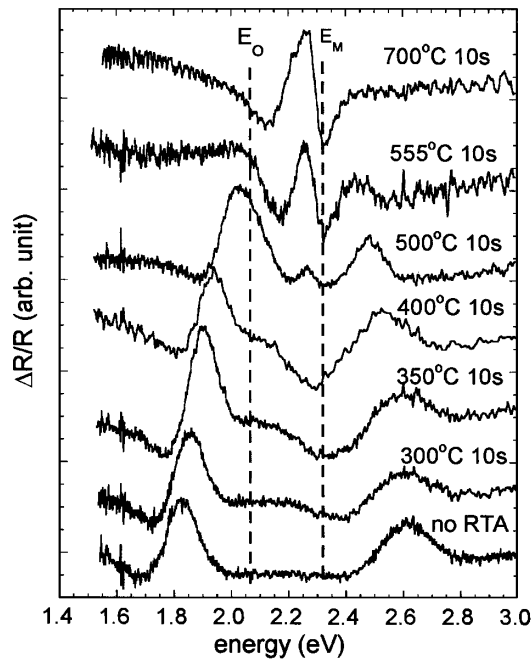


FIG. 2. PR spectra from  $Zn_{0.88}Mn_{0.12}Te$  samples implanted with 3.3% O followed by PLM with  $0.15 J/cm^2$  and rapid thermal annealing (RTA) for 10 sec at annealing temperatures from 300–700 °C.

PLM with different energy fluences. We note here that  $x$  decreases with increasing energy fluence higher than the melt threshold ( $\sim 0.08 J/cm^2$ ), possibly due to the longer melt duration and/or dilution through the deeper melt depth. The energy positions of the two transitions as predicted by the BAC model are plotted as solid lines.

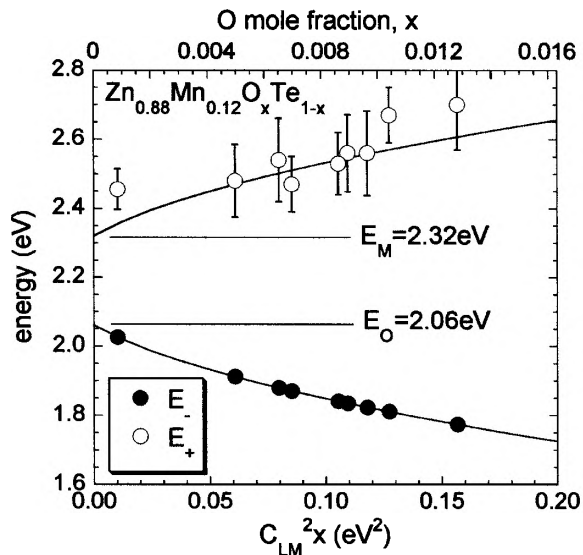


FIG. 3. The energy positions of  $E_-$  and  $E_+$  for the  $Zn_{0.88}Mn_{0.12}O_xTe_{1-x}$  alloys plotted against the O mole fractions  $x$ . The values of  $E_-$  and  $E_+$  calculated according to the band anticrossing model are plotted as solid lines.

Here, since the values of  $x$  were calculated from the  $E_-$  transition no error bars are given for  $E_-$ . Given the broad linewidths of the  $E_+$  transitions, they agree reasonably well with the calculated values for samples with various O mole fractions.

The new diluted II-VI oxide has technological potentials for photovoltaic applications. Efforts to improve the efficiency of solar cells have led to extensive experimental and theoretical studies of new materials and cell designs. To date, the highest power conversion efficiency of  $\sim 33\%$  have been achieved with multijunction solar cells based on standard semiconductor materials [16–18]. It was recognized over 30 years ago that the introduction of states in a semiconductor band gap presents an alternative to multijunction designs for improving the power conversion efficiency of solar cells [19–21]. It was argued that deep impurity or defect states could play the role of the intermediate states for this purpose. Detailed theoretical calculations indicate that a single-junction cell with one and two properly located bands of intermediate states could achieve power conversion efficiencies up to 62% [20] and 71.7% [21], respectively. However, difficulties in controlling the incorporation of high concentrations of impurity or defect states have thwarted prior efforts to realize such materials.

With multiple band gaps that fall within the solar energy spectrum,  $Zn_{1-y}Mn_yO_xTe_{1-x}$  provides a unique opportunity for the assessment of the proposed multi-band solar cell. The energy band structure and the density of states for the case of  $Zn_{0.88}Mn_{0.12}O_xTe_{1-x}$  alloy (with  $x \sim 0.01$ ) are shown in Fig. 4. An O derived narrow band of extended states  $E_-$  is separated from the upper subband  $E_+$  by about 0.7 eV. Three types of optical

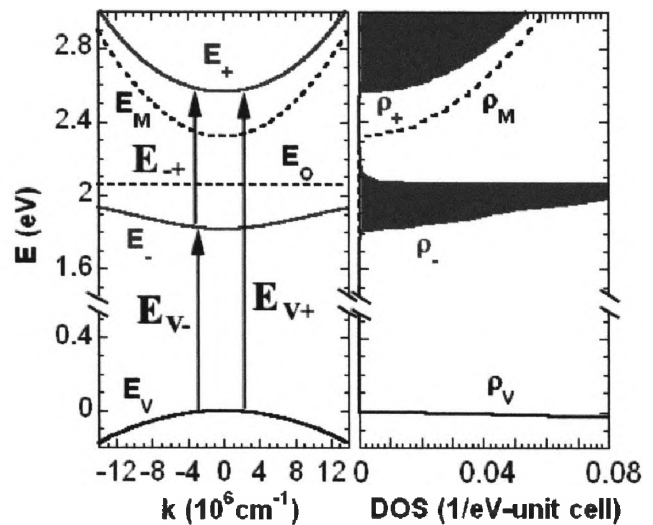


FIG. 4. The calculated energy band structure (left panel) and density of states (right panel) for  $Zn_{0.88}Mn_{0.12}O_xTe_{1-x}$  with  $x \sim 0.01$ . The three possible optical transitions are indicated in the left panel.

transitions are possible in this band structure: (i) from the valence band to the  $E_+$  subband,  $E_{V+} = E_+(k=0) - E_V(k=0) = 2.56$  eV; (ii) from the valence band to  $E_-$  subband,  $E_{V-} = E_-(k=0) - E_V(k=0) = 1.83$  eV; and (iii) from  $E_-$  to  $E_+$ ,  $E_{+-} = E_+(k=0) - E_-(k=0) = 0.73$  eV. These three absorption edges span much of the solar spectrum, thus these alloys are good candidates for the multiband semiconductors envisioned for high efficiency photovoltaic devices.

To further evaluate the suitability of the  $\text{Zn}_{0.88}\text{Mn}_{0.12}\text{O}_x\text{Te}_{1-x}$  HMAs for solar cell applications we have calculated the solar cell power conversion efficiency for the material with the electronic band structure shown in Fig. 4. The calculations are based on the implementation of the detailed balance theory [22] to the case of a three-band semiconductor [20,21]. Even for this nonoptimal band gap configuration we calculate a power conversion efficiency of 45%, which is higher than the ideal efficiency of any solar cell based on a single-junction in a single-gap semiconductor and is comparable to the efficiency of triple-junction cells. Increasing  $x$  in  $\text{Zn}_{0.88}\text{Mn}_{0.12}\text{O}_x\text{Te}_{1-x}$  to slightly above 0.02 would increase the gap between  $E_+$  and  $E_-$  to 1 eV and leads to an optimum power conversion efficiency of 56%.

In conclusion, we have synthesized  $\text{Zn}_{1-y}\text{Mn}_y\text{O}_x\text{Te}_{1-x}$  ternary ( $y = 0$ ) and quaternary ( $y = 0.12$ ) alloys by  $\text{O}^+$  implantation followed by pulsed laser melting. Alloys with substitutional O mole fraction in the Te sublattice as high as 0.012 have been achieved. Optical transitions corresponding to both the lower ( $E_-$ ) and upper ( $E_+$ ) conduction subbands resulting from the anticrossing interaction between the localized O states and the extended conduction states of the matrix are clearly observed in these diluted II-VI oxides. We demonstrate that these alloys fulfill the criteria for three-band semiconductor that has been proposed as a means of making high efficiency, single-junction solar cells. We note that the great advantage of this material system is that further optimization of solar cell performance can be achieved by varying the alloy composition, changing the Mn content or replacing Mn with Mg.

This work was supported by the Director, Office of Science, Office of Basic Energy Sciences, Division of Materials Sciences and Engineering, of the U.S. Department of Energy under Contract No. DE-AC03-76SF00098. M. A. S. acknowledges support from NSF.

- [1] See, for example, Special Issue: III-N-V Semiconductor Alloys [Semicond. Sci. Technol. **17**, 741 (2002)].  
 [2] K. M. Yu, W. Walukiewicz, J. Wu, J. W. Beeman, J. W. Ager, E. E. Haller, I. Miotkowski, A. K. Ramdas, and P. Becla, Appl. Phys. Lett. **80**, 1571 (2002).

- [3] W. Shan, W. Walukiewicz, J. W. Ager III, E. E. Haller, J. F. Geisz, D. J. Friedman, J. M. Olson, and S. R. Kurtz, Phys. Rev. Lett. **82**, 1221 (1999).  
 [4] W. Walukiewicz, W. Shan, K. M. Yu, J. W. Ager III, E. E. Haller, I. Miotkowski, M. J. Seong, H. Alawadhi, and A. K. Ramdas, Phys. Rev. Lett. **85**, 1552 (2000).  
 [5] J. Wu, W. Shan, and W. Walukiewicz, Semicond. Sci. Technol. **17**, 860 (2002).  
 [6] W. Walukiewicz, W. Shan, J. W. Ager III, D. R. Chamberlin, E. E. Haller, J. F. Geisz, D. J. Friedman, J. M. Olson, and S. R. Kurtz, in *Photovoltaics for the 21st Century*, edited by V. K. Kapur, R. D. McDonnell, D. Carlson, G. P. Ceasar, and A. Rohatgi (Electrochemical Society Press, Pennington, 1999) p. 190.  
 [7] C. Skierbiszewski, P. Perlin, P. Wiśniewski, W. Knap, T. Suski, W. Walukiewicz, W. Shan, K. M. Yu, J. W. Ager, E. E. Haller, J. F. Geisz, and J. M. Olson, Appl. Phys. Lett. **76**, 2409 (2000).  
 [8] K. M. Yu, W. Walukiewicz, W. Shan, J. W. Ager III, J. Wu, E. E. Haller, J. F. Geisz, D. J. Friedman, J. M. Olson, and Sarah R. Kurtz, Phys. Rev. B **61**, R13337 (2000).  
 [9] *Laser and Electron Beam Processing of Materials*, edited by C. W. White and P. S. Peercy (Academic Press, New York, 1980).  
 [10] J. S. Williams, in *Laser Annealing of Semiconductors*, edited by J. M. Poate and J. W. Mayer (Academic Press, New York, 1982), p. 385.  
 [11] K. M. Yu, W. Walukiewicz, J. W. Beeman, M. A. Scarpulla, O. Dubon, M. R. Pillai, and M. Aziz, Appl. Phys. Lett. **80**, 3958 (2002).  
 [12] K. M. Yu, W. Walukiewicz, M. A. Scarpulla, O. D. Dubon, J. Jasinski, Z. Liliental-Weber, J. Wu, J. W. Beeman, M. R. Pillai, and M. J. Aziz, J. Appl. Phys. **94**, 1043 (2003).  
 [13] M. A. Scarpulla, K. M. Yu, O. Monteiro, M. Pillai, M. C. Ridgway, M. J. Aziz, and O. D. Dubon, Appl. Phys. Lett. **82**, 1251 (2003).  
 [14] D. E. Aspnes, Surf. Sci. **37**, 418 (1973).  
 [15] M. J. Seong, H. Alawadhi, I. Miotkowski, A. K. Ramdas, and S. Miotkowska, Phys. Rev. B **60**, R16275 (1999).  
 [16] P. K. Chiang, J. H. Ermer, W. T. Nishikawa, D. D. Krut, D. E. Joslin, J. W. Eldredge, B. T. Cavicchi, and J. M. Olson, in *Proceedings of the 25th IEEE Photovoltaic Specialists Conference* (IEEE, New York, 1996), p. 183.  
 [17] S. R. Kurtz, D. Myers, and J. M. Olson, in *Proceedings of the 26th IEEE Photovoltaic Specialists Conference* (IEEE, New York, 1997), p. 875.  
 [18] R. R. King, P. C. Coffey, D. E. Joslin, K. M. Edmondson, D. D. Krut, N. H. Karam, and Sarah Kurtz, in *Proceedings of the 29th IEEE Photovoltaic Specialists Conference, New Orleans, 2002* (IEEE, New York, 2002), pp. 852–855.  
 [19] M. Wolf, Proc. IRE **48**, 1246 (1960).  
 [20] A. Luque and A. Marti, Phys. Rev. Lett. **78**, 5014 (1997).  
 [21] A. S. Brown, M. A. Green, and R. P. Corkish, Physica E (Amsterdam) **14**, 121 (2002).  
 [22] W. Shockley and H. J. Queisser, J. Appl. Phys. **32**, 510 (1961).